Temperature-Triggered Failure Hazard Mitigation of Transformers Subject to Geomagnetic Disturbances

Pooria Dehghanian, *Student Member*, *IEEE,* and Thomas J. Overbye, *Fellow*, *IEEE*
Department of Electrical and Computer Engineering, Texas A&M University, College Station, Texas, USA
{pooria.dehghanian; overbye}@tamu.edu

***Abstract*— Geomagnetic Disturbances (GMDs) could potentially damage the power grid through reactive power losses and overheating the high-voltage power transformers. A high-impact Low-frequency event such as GMD could induce a hotspot temperature rise over the transformer's overall temperature during a full load condition leading to an accelerated asset loss of life and increased risk of failure. This paper focuses on the impact of GMDs on transformers heating and its consequences on transformer's loss of life cycle and failure risk. Moreover, this paper proposes a transformer hazard mitigation approach to reduce the temperature-dependent transformer risk of failure. The proposed method is tested in the synthetic Texas 2000-bus grid, and the results are numerically analysed, demonstrating the effectiveness of the algorithm.**

***Index Terms*— Geomagnetic disturbances (GMDs); Hotspot temperature; Hazard of failure; Geomagnetic induced current (GIC); Mitigation, Transformer, Loss of life.**

I. NOMENCLATURE

A. Variables

α	Transformer turn ratio
θ_{ss}	Steady-state temperature
θ_i , θ_F	The initial and final temperature
θ_{HS}	GIC-caused hotspot temperature rise
θ_{oil}	Temperature of oil
$\theta_{Ambient}$	Average ambient temperature
$\Delta\theta_{H,full\_load}$	Winding Hotspot temperature under full load condition
$\Delta\theta_{to}$	Top-oil rise over the ambient temperature
$\Delta\theta_h$	Winding hotspot rise over top-oil temperature
P_r	Probability of transformer failure
λ	Arrhenius rate
I_H , I_L	dc current at the high and low side of the transformer
t	Time
H	Failure hazard rate
K_u	The ratio of ultimate load to rated load
R	The ratio of load loss between rated load and no-load
$\mathbf{I}_{dc}^T$	Total dc current flowing through transformers
$\mathbf{V}=[V_1,...,V_n]^T$	dc voltage at any bus and substation neutral

B. Parameters

E_N , E_E	Northward and Eastward geoelectric field (V/km) components
$\mathbf{G}$	Network conductance matrix
τ	Thermal time constant
$L_N(n,m)$ $L_E(n,m)$	Northward and Eastward distance for a transmission line connecting bus *m* and bus *n*.
τ_w , τ_{to}	The thermal time constant of winding and oil
A, B	The constant value of Weibull distribution
β	the shape parameter of Arrenhius distribution function
E_a	Activation Energy (ev)

C. Indices

T_{AA}	Transformer's age acceleration factor
T_A^{EQ}	Transformer's equivalent aging factor

D. Functions

$f(t)$	Probability of density distribution function
$F(t)$	Cumulative distribution function
$h(t)$	Impulse response function

E. Abbreviations

ini	Refers to initiate value
ult	Refers to ultimate value
GIC	Refers to Geomagnetically Induced Current
GMD	Refers to Geomagnetic Disturbance

II. INTRODUCTION

GEOMAGNETIC DISTURBANCES (GMDS) are solar-driven incidents that could cause catastrophic impacts on various parts of power grids. Solar storms and coronal mass ejections potentially cause variations in Earth's magnetic field, which induce low-frequency electric fields on the surface of the earth. These changes in the magnetic field produce geomagnetically induced currents (GICs) flowing into high-voltage transmission lines. Although GICs are typically relatively lower frequency currents within the range of [0.1-100 mHz], they yield quasi-dc impacts with potentially detrimental consequences in the power grid and especially in high-voltage power transformers [1], [2].

Typically, two main issues arise in a GMD event based on the intensity of the injected GICs: a) excessive reactive power consumption due to loss of magnetic flux and a local voltage drop accordingly, b) transformer's core and winding overheating. Such induced currents intensify the temperature rise of windings and metallic parts of transformers through damaging the insulation parts of transformers. In the worst-case GMD incident, these detrimental effects can appear together, leading to system-wide disruptions and even possible blackouts due to the loss of high-voltage power transformers. An example is the 8-hour GMD-driven blackout of the Hydro-Quebec power system in March 1989, which left nine million people out of

electricity—one of the largest outages due to a GMD incident in history [3]. Hence, continuous monitoring and situational awareness and implementing practical solutions to mitigate the GIC impacts on the power grid are urgently needed.

While it is difficult to predict which parts of the power system would be affected by GMD before the incident, determining its formation and impacts on power grid critical assets can provide insightful clues to the power grid planners and operators. Some works of literature have been conducted to model [4], [5], monitor [6], control [7], and mitigate [8] the impacts of GICs on the power grid. Some other research projects have been reported on the impact of GICs on transformer's harmonics, reactive power losses, and heating [9]-[11].

Apart from the previous literature, this paper focuses on the mitigation of temperature-triggered transformer's hazard of failure following a GMD disturbance. The main contributions of the paper are: a) deriving temperature models of transformers during a GMD hotspot and under full load conditions; b) quantifying the loss of life and failure risk of transformers triggered by a GMD disturbance; c) mitigating the transformer's hazard of failure through reducing the loading of the transformer. The above approach is tested in the Texas 2000-bus synthetic case, and the results verify the effectiveness of the algorithm.

The rest of the paper is organized as follows. GIC modeling and its characteristics are presented in Section III. The transformer's thermal model and its behavior are discussed in Section IV. Section V includes the hazard of failure mitigation and the transformer's loss of life formulation. The case study and simulation results are illustrated in Section VI. The paper ends with the conclusion in Section VII.

III. GIC Modelling and Characteristics

A. Geophysical Parameter Consideration for GIC Characterization

Several parameters need to be considered in deriving an appropriate GIC model such as geomagnetic latitude/longitude (B-field), ground conductivity, power network topology, and geoelectric field (E-field) magnitude and orientation, line resistance, transmission line length, and its orientation alignment corresponding with E-field, etc. [12]. Moreover, the design and characteristics of transformers, especially the core type, impact GIC-damage severity. According to the literature, a transformer with a single-phase core is more GIC-caused saturation vulnerable than a 3-phase one when they are injected to the same level of GIC magnitude [13].

B. GIC Modelling in DC Network Analysis

The following are the procedures to obtain the GIC value with the assumption of a uniform electric field distribution across the network. As described earlier, coronal mass ejection changes the magnetic field of the surface of the Earth, which, itself, induces a voltage potential on the transmission lines. It can be calculated by integrating the E-field through the length of the line. From dc perspective analysis, for a uniform E-field, the induced dc voltage can be calculated as [14], [15]:

$$V(n,m) = E_N\ L_N(n,m) + E_E\ L_E(n,m) \tag{1}$$

Then, using the Norton Equivalent model, the dc voltage is converted to the dc current injection. The total dc injected current I_{dc} is calculated via Kirchhoff's current law and considering the total effective resistance R_{eff}, such as the resistances of the line, substation grounding, and transformer's winding shown in (2) and (3).

$$I_{dc} = I(n,m) = \frac{V(n,m)}{R_{Eff}} = \sum_{(n,m)} \left(\frac{1}{R_{Eff}} \left(E_N\ L_N(n,m) + E_E\ L_E(n,m) \right) \right) \tag{2}$$

$$\mathbf{V} = \mathbf{G}^{-1}\ \mathbf{I}_{\mathrm{dc}} \tag{3}$$

The GIC current flow I_{nm}, passing through the transformers between busses *n* and *m* can be obtained as follows:

$$\mathbf{I}_{nm}^{T} = \mathbf{G}_{\mathrm{nm}} .(\mathbf{V}_{\mathrm{n}} - \mathbf{V}_{\mathrm{m}}), \quad \forall n \in \Omega_B, \forall m \in \Omega_S \tag{4}$$

where Ω_B and Ω_S are the sets of network buses and substations, respectively. Finally, due to the linear relationship between the GIC current and geoelectric field (E), the transformer GIC will be

$$\mathbf{I}_{dc}^{T} = \mathbf{G}_{\mathrm{total}} \sum_{n \in N} \frac{L(n,m)}{R_{Eff}(n,m)} .\mathbf{E} \tag{5}$$

$I_{effective}^{GIC}$ plays an important role when injected into the transformer's winding. It is the effective per phase current depending on the transformer turn ratio and configuration. It depends on the current in both coils in autotransformers, and wye-grounded-wye transformers since both the low and the high side of the transformer pass the current. However, for a GSU transformer and wye grounded-delta transformers, $I_{effective}^{GIC}$ is the current in the high-side (grounded) winding [16]. The per phase $I_{effective}^{GIC}$ can be obtained using (6).

$$I_{effective}^{GIC} = \left| \frac{\alpha I_H + I_L}{\alpha} \right| = \left| I_H + (\frac{I_N}{3} - I_H)\ V_L \middle/ V_H \right| \tag{6}$$

IV. Transformer Temperature Model and Formulation

Due to the dynamic nature of the temperature deviations, it is important to carefully assess the thermal stress on power transformers during a GMD event. Nowadays, most of the transformers are equipped with thermal sensors; however, due to aging or any sudden damage to sensors, the measurement might be inaccurate. Thus, it is necessary to come up with an approximation of the thermal model. Oil, windings, and metallic segments are the main transformer's thermal-stressed elements that need to be taken care of [17]. Besides, ambient temperature is another variable that influences the total temperature of a transformer.

According to the NERC, the tie plate is more sensitive to temperature rise than the winding and is more susceptible to be thermally damaged. Usually, oil has a much larger thermal constant than the other parameters, though its variation is relatively low.

A. GIC-Caused Temperature Rise Model

Estimating the thermal response of a transformer corresponding to injected GIC input is achievable using the test measurement data or manufacturer calculations. In so doing, the trend of the transformer's temperature corresponding to a constant injected current is monitored. Fig. 1 shows that the temperature deviates exponentially for a given constant current, and Fig. 2 illustrates the transformer's asymptotic steady-state hotspot temperature variation vs. various GIC injection [18]. As it can be observed from Fig. 1 and Fig. 2, the steady-state thermal response of the transformer corresponding to various level of constant injected GICs can be linearly approximated and modeled as follows. Due to the time-invariant nature of the steady-state hotspot temperature to a given constant current (see Fig. 2), the linear time-invariant (LTI) heating model can be

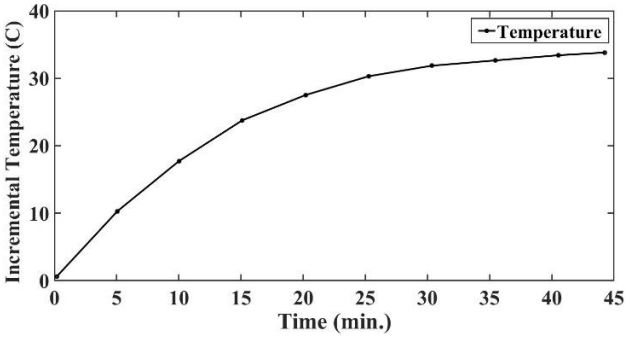

Fig. 1. Transformer's thermal step unit behavior to a 16.67 A/phase GIC.

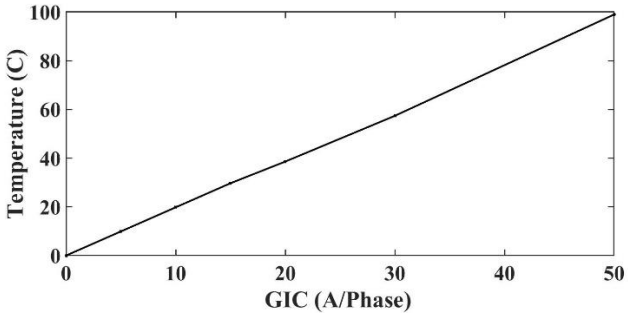

Fig. 2. Asymptotic steady-state hotspot temperature vs. GIC.

$$\begin{cases} \Delta\theta(t) = \theta_{ss}(1-\sum_{i=1}^{n} c_i e^{-t/\tau_i}) \\ \theta_{ss} = \Delta\theta_F - \Delta\theta_i \end{cases} \tag{7}$$

$$\begin{cases} \lim_{t\to\infty} \Delta\theta(t) = \theta_{ss} \\ \Delta\theta(t) = 0 \qquad \forall t < 0 \end{cases} \tag{8}$$

found through the impulse response of the system by the derivative of the step response (7), as shown in (9) [19].

$$\Delta\theta_h(t) = \sum_{i=1}^{n} \frac{\theta_{ss} c_i}{\tau_i} e^{-\frac{t}{\tau_i}} = h(t) \tag{9}$$

Finally, the hotspot temperature of a transformer can be derived through convolution of the input signal [i.e., GIC(t)] and the thermal impulse response $h(t)$ as follows:

$$\Delta\theta_{HS}(t) = GIC(t) * h(t) \tag{10}$$

The above thermal model can approximate the temperature rise of winding and tie plates if the thermal time constant τ is known. The final temperature of the transformer would be calculated through the summation of the hotspot temperature, oil temperature, and ambient temperature, as presented in (11).

$$\theta_{Final}(t) = \theta_{HS} + \theta_{oil} + \theta_{Ambient} \tag{11}$$

According to the IEEE standard [20], the threshold of the transformer's total temperature for long-term operation at rated load is 110 °C while the average and maximum temperature rise above the ambient temperature for the winding alone is 65 °C and 80 °C, respectively. However, the short-time hotspot temperature of the transformer (including oil and ambient temperature) under full load conditions should not exceed 200 °C.

B. Transformer Temperature under full-Load Conditions

As thoroughly explained in IEEE Standard C57.91 [20], the thermal stress of transformers under a full-load condition can be calculated as follows:

$$\Delta\theta_{H,full\_load} = \Delta\theta_{to} + \Delta\theta_h + \Delta\theta_{ambient} \tag{12}$$

where,

$$\Delta\theta_h = (\Delta\theta_{h,ult} - \Delta\theta_{h,ini}) \,.\, (1 - e^{-\frac{t}{\tau_w}}) + \Delta\theta_{h,ini} \tag{13}$$

$$\Delta\theta_{to} = (\Delta\theta_{to,ult} - \Delta\theta_{to,ini}) \,.\, (1 - e^{-\frac{t}{\tau_{to}}}) + \Delta\theta_{to,ini} \tag{14}$$

The ultimate hotspot rise over top oil and top oil rise over temperature are as follows:

$$\Delta\theta_{h,ult} = K_u^{2m} \,.\, \Delta\theta_{h,rated\_load} \tag{15}$$

$$\Delta\theta_{to,ult} = \left[\frac{(K_u R + 1)}{(R+1)}\right]^n \,.\, \Delta\theta_{to,rated\_load} \tag{16}$$

In the above equations, m and n are the empirical values determined by the type of transformers.

V. Transformer's Hazard of Failure and Loss of Life Mitigation

The dc-GIC value may push forward a transformer to its saturation mode and increase the temperature inside of the transformer. As a result, the major consequences of this overheating would be increased in transformer loss of life and its failure hazard rate. The formulations and mitigation procedures are described in this section as follows.

A. Transformer Life-Time Assessment Metric

A couple of time-varying factors influence transformer failure insulation, such as temperature, moisture, and oxygen content. Although a perfect assessment of the loss of transformer's insulation life is challenging, due to the recent high-accurate technologies in gas and oil preservation, the non-uniform temperature distribution across the windings and tie-plates is considered as the main factor influences the transformer's loss of life cycle. It should be continuously taken care of [21]-[23].

The age acceleration factor can be utilized as a metric to identify the most thermally vulnerable transformers and is formulated as follows:

$$T_{AA} = EXP\left(\frac{1500}{383} - \frac{1500}{\theta_{Final} + 273}\right) \tag{17}$$

While,

$$\begin{cases} T_{AA} > 1 & if \;\; \theta_{Final} > 110\ ^0C \\ T_{AA} = 1 & if \;\; \theta_{Final} = 110\ ^0C \\ T_{AA} < 1 & if \;\; \theta_{Final} < 110\ ^0C \end{cases} \tag{18}$$

The T_{AA} indicates the transformer's degree or rate of aging acceleration for the temperature above the reference temperature of 110 °C. In other words, an aging factor, e.g., 10 for a transformer with a hotspot temperature of 140 °C, means that one hour in this condition is equivalent to 10 hours at the rated temperature of 110 °C.

The equivalent aging factor is determined as follows:

$$T_A^{EQ} = \frac{\sum_{t=1}^{T}\left[EXP\left(\frac{1500}{383} - \frac{1500}{\theta_{Final}+273}\right)\right] * \Delta t}{\sum_{t=1}^{T} \Delta t} \tag{19}$$

In our simulations, Δt is set to be a 10-second time-step to represent better the dynamic change of temperature rise and, thus, to minimize the age factor error. The total simulation time is 31 h. Finally, the transformer loss of life percentage can be assessed by using the rate of age acceleration (17) and equivalent age factor (19) as formulated in (20):

$$\% \; T_{Life\ Loss} = \frac{T_A^{EQ} * Simulation\ Time}{Normal\ Life} * 100 \qquad (20)$$

Note that the typical transformer insulation life is about 20-21 years (i.e., 180000 h).

B. Hazard of Failure Formulation using the Arrhenius-Weibull Reliability Model

The failure rate function is one of the indices that RCM practitioners and maintenance engineers use to do asset management and prioritization. The hazard function is not a probability but is indeed a rate or a measure of risk in which the greater the hazard at an interval, the higher the risk of failure at that time. In other words, it is the expected number of events a device can expect per time unit conditional on being at risk of failure, given that it has not failed before.

GIC-caused hotspot temperature might put stress on the dielectric insulation of the transformer and increases its probability of failure. As it is recommended by the IEEE standard, Weibull distribution can be used to measure the reliability of the electrical components, which depends on the number of operation hours and age of devices. Therefore, in this paper, the Arrhenius-Weibull model is used to quantify the hazard of failure of the transformer caused by accelerated thermal stress [22]. The probability of transformer failure is shown in (21), and the hazard function presented in (22) is used to approximate (21) when t_0 and t_1 are close enough.

$$P_r(t_0 < T \le t_1 \mid T > t_0, \theta) = \frac{P_r(t_0 < T \le t_1 \mid \theta)}{1 - P_r(T \le t_0 \mid \theta)} \qquad (21)$$

where $\Delta t = t_1 - t_0$ and $H(t_0 \mid \theta)$ is the Hazard function, which is defined and calculated as

$$\begin{cases} P_r(t_0 < T \le t_1 \mid T > t_0, \theta) = H(t_0 \mid \theta) \; . \; \Delta t \\ H(t_0 \mid \theta) = \dfrac{f(t_0)}{1 - F(t_0)} \end{cases} \qquad (22)$$

The Arrhenius-Weibull reliability distribution model is used to fit the probability density function $f(t_0)$ and cumulative distribution function $F(t_0)$ to the thermal stress model of the transformer as follows:

$$f(t) = \frac{\beta}{\lambda}\left(\frac{t}{\lambda}\right)^{\beta-1} e^{\left(-\frac{t}{\lambda}\right)^{\beta}} \qquad (23)$$

$$F(t) = 1 - e^{\left(-\frac{t}{\beta}\right)^{\lambda}} \qquad (24)$$

$$\lambda = A.e^{\left(\frac{B}{\theta_H + 273}\right)} \qquad (25)$$

$$B = \frac{E_a}{k} \qquad (26)$$

where β is the shape parameter of the Weibull model and is obtained from historical failure data of transformers. If $\beta > 1$ the failure rate increases. The parameter B can be calculated if the activation energy E_a is given; otherwise, it can be estimated through historical data.

C. Proposed Hazard Mitigation Algorithm

Hazard mitigation procedures are as follows:

Algorithm: Hazard Calculation

1: Solve GIC flow
2: Calculate the transformer's GIC-caused temperature rise ($\theta_{HS}(I)$) and the hotspot temperature under loading condition ($\Delta\theta_{H,full\_load}$)
3: Identify the overheated transformers
4: Calculate the loss of life of transformers and hazard of failure ($H(\theta_{HS}, I)$)

Hazard Mitigation Procedure

5: Set the desired threshold for hazard rate as H_{Th}
6: Initialize the transformer load rate, line power flow, load shed step size, simulation time, etc.
7: while $H > H_{Th}$ & (Load- load shed >0)
8: Reduce the $Load(\theta, I)$ by step size
9: Perform recursive step 2 ($\theta_{HS}(I)$) & step 4 ($H(\theta_{HS}, I)$)
10: end procedure

VI. Case Studies And Numerical Simulations

The suggested approach is tested through a Texas 2000-bus synthetic test system. The input of the developed GIC model is a time-series historical electric field data derived from the 31-hour of GMD event on March 13, 1989. Note that the studied time-variant E-field used to estimate GIC(t) is in the form of a uniform space spectral across the system and is sampled at a 10s time resolution. The peak of the E-field value is 8 V/km. Having transformed the E-field series to the effective GIC values using (1)-(6), the GIC(t) will be applied to the heating model described in Section IV. The thermal time constant is derived from Fig.1 and is set to 770 s.

A. Analyze of GIC vs. Temperature during the Simulation

The test system is composed of 2000 buses, 861 transformers, 3206 transmission lines, 544 generating units, and 1350 load points. According to the NERC report [18], the transformers which are facing the GIC above 75 A/phase are more vulnerable to get thermally damaged, and hence, must be determined and carefully assessed further. The transformers affected by GICs less than 75 A/phase can be assigned a lower priority for condition assessment and possible maintenance considerations. Fig. 3 illustrates a list of network transformers that experience at least one instance of the peak GIC value higher than 75 A/phase. Their corresponding maximum GIC-caused temperature magnitude is presented in Fig. 4.

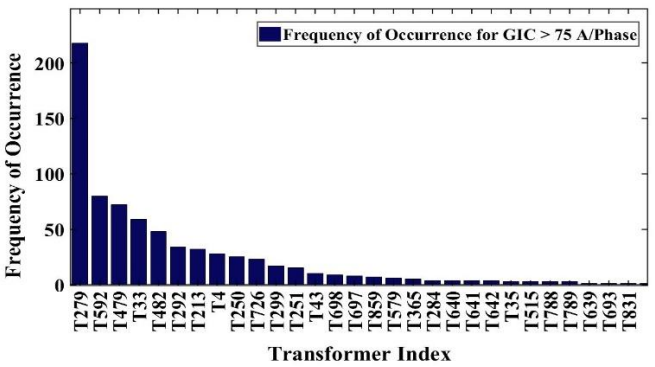

Fig. 3. The frequency of occurrence a transformer experiencing GIC > 75 A/Phase.

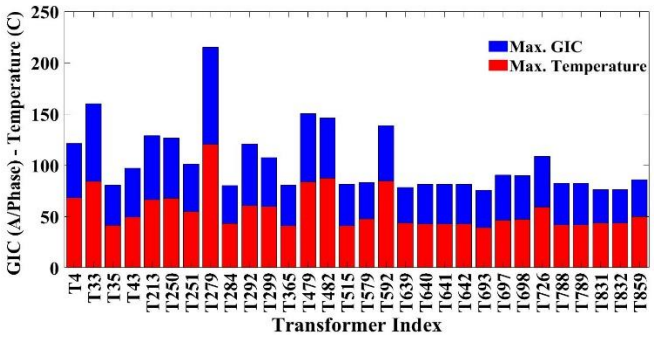

Fig. 4. The most vulnerable transformers and the corresponding GIC-caused maximum temperature.

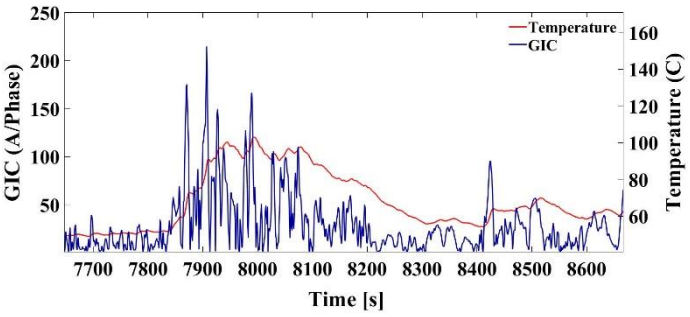

Fig. 5. Transformer 279 tie-plate GIC-temperature rise over time in reference 8 V/km event.

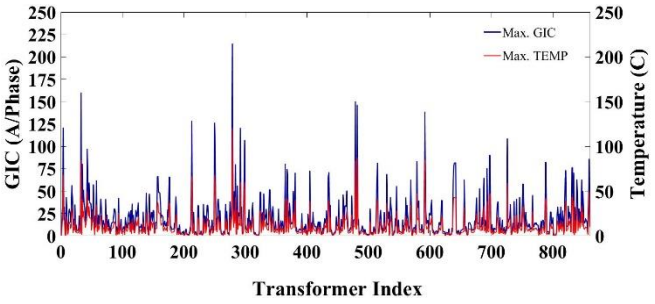

Fig. 6. Maximum GIC and its corresponding temperature rise on all transformers across the network.

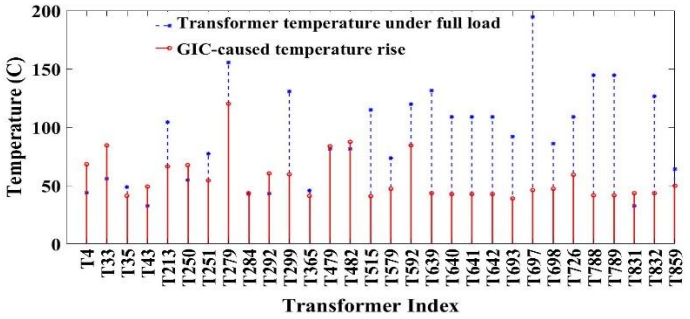

Fig. 7. Transformer thermal response with and with no presence of GIC.

Zooming into a portion of the event, Fig. 5 focuses on T279 (where the temperature is observed to be at the highest) and reveals that the temperature rise reaches a maximum of 120.24 °C. Fig. 6 displays the maximum GICs and their corresponding temperature appearing on various transformers across the 2000-bus synthetic power grid. The highest peak GIC of 214.86 (A/phase) and the maximum temperature rise of ~120.24 °C are recorded on transformer T279. Moreover, The Gic-caused hotspot temperature of transformers during the full load condition before the GMD event is calculated using (12)-(16). It is demonstrated in Fig.7, where one can compare the GIC-caused temperature rise vs. hotspot temperature under full load before the presence of GMD. Note that the average ambient temperature is set to 25 °C.

B. *Transformer Loss of Life Estimation*

The impact of thermal stress caused by GMD on the loss of life probability of transformers is investigated. The loss of life indicates the transformers' equivalent life cycle (in hours) in a given time interval (here about 31 hours) that will be exposed at the reference temperature (110 °C). Take Fig. 8 as an example in which illustrates the loss of life of transformers under loading conditions in the presence of GMD. The percentage of loss of life for T279 is 0.032%. It is equivalent to the loss of life of the transformer if it remains at the reference temperature of 110 °C for 1 hour.

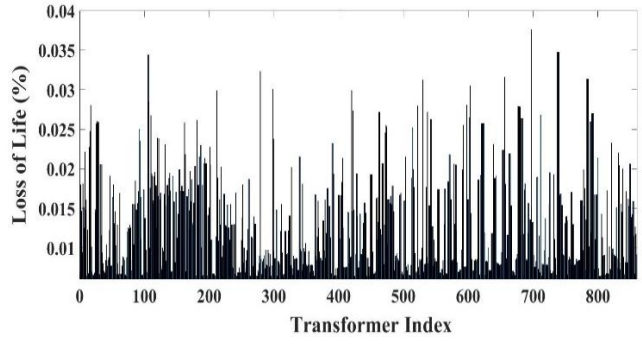

Fig. 8. The percentage of loss of life for different transformers.

C. *Analyze of Transformer's Hazard of Failure*

According to the hazard definition, hazard is the rate of a device failure at the time $t+\Delta t$ given that it has not been failed before time t . The hazard rate of transformers considering only the GIC-caused temperature rise is calculated using (15)-(20) and are shown in Fig. 9. The parameter β is set to 1.26 from historical data. The parameter t of the hazard function is the time that each transformer violates the temperature threshold of 110 °C (during normal operating conditions) for the first time, which temperature fluctuates above the threshold for a considerable time. Take T35 as an example. This transformer is overheated for more than 30 minutes. The hazard rate is 0.35, meaning that the probability rate of failure within the next hour is 0.35 assuming the hazard remains constant during that hour.

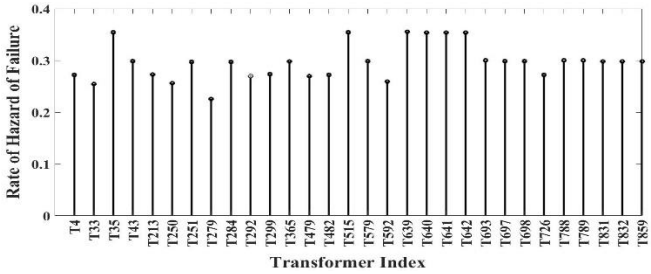

Fig. 9. The hazard of the failure rate of vulnerable transformers corresponds to the reference temperature of 110 C.

D. *Mitigating the Transformer's hazard of Failure risk*

In this paper, the main purpose of analyzing the transformer hazard rate is to find the high-risk transformers and provide mitigation solutions to reduce the hazard rate. Since the hazard rate is a function of temperature, which itself is a function of current, one way to reduce the hazard rate is to shed the load of high-risk transformers. Decreasing the loading of transformers reduces the transformer's temperature under full loading conditions and mitigates the hazard rate value of the transformer within a safe range. In this paper, the desired hazard rate threshold is set to 0.35, meaning that transformers are almost operating in a safe zone if the hazard is less than 0.35.

TABLE I
TRANSFORMER HAZARD OF FAILURE MITIGATION DURING GMD EVENT

T_{Index}	Before Mitigation			After Mitigation		
	H	Load (MVA)	θ_{full_Load}	H	Load (MVA)	θ_{full_Load}
T279	0.6911	1102	155.48	0.35	981	132.2
T298	0.9055	1211	165.56	0.35	1119	147.92
T530	0.7696	104	170.55	0.35	94	147.5
T656	0.9066	190	172.68	0.35	170	147.24
T697	0.5379	184	194.57	0.35	150	144.86

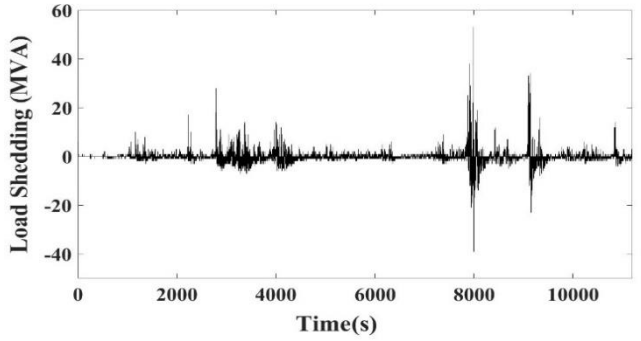

Fig. 10. Time-series load shedding for failure mitigation of T279.

From the thermal analysis of transformers, the total hotspot temperature of a total of 5 transformers exceeds the IEEE standard of 200 °C during a short period of full-load operation. In order to mitigate their hazard of failure rate, the load shedding plan is executed with the step size of 1 MVA until the hazard rates are less than the user-defined threshold (here 0.35). Through implementing the algorithm described in Section V, the effectiveness of the hazard mitigation can be seen in Table I, where T_{Index} is the transformer index. $\theta_{H,full\_Load}$ is the hotspot temperature under full load, and the load (MVA) is the amount of power passing through the line connected to the transformer. Table I indicates that, for example, to reduce the probability of failure of T279 from 0.69 to 0.35, the transformer temperature under loading condition should drop from 155 °C to 132 °C. To reduce the temperature, the operator should shed the load power in a timely manner from the initial 1102 MVA to 850 MVA, as shown in Fig.10.

Fig. 10 shows the timely-manner load shed step that should be done to keep the transformer failure rate to 0.35. Note that both GIC and temperature are changing each time. The negative amount of load shedding at different time points is because of fluctuations of GIC and its corresponding temperature rise at those time points. It means that some of the shed load can be restored back to the system while the hazard is still less than the threshold.

VII. CONCLUSION

This paper proposes a temperature-dependent transformer's hazard of failure assessment and presents a mitigation solution for reducing the risk of failure of transformers following a GMD. In so doing, first, two separate heating models of transformers are suggested in which one model approximates the asymptotic GIC-caused temperature rise of transformers, and the other calculates the transformer temperature under full load condition when no GMD hit the system. Then, using the derived GIC model, the transformer loss of life is calculated. The risk of transformer failure is modeled and calculated using the Arrhenius-Weibull distribution probability function. Finally, the rate of failure of high-risked transformers is mitigated through controlling the transformer load power. The effectiveness of the approach, as mentioned above, is tested and verified using the synthetic Texas 2000-bus case.

ACKNOWLEDGMENT

This project was funded in part by the National Science Foundation (NSF) Award Number: NSF 15-20864.

REFERENCES

[1] F. Aboura and O. Touhami, "Effect of the GICs on magnetic saturation of asymmetric three-phase transformer," *IET Electr. Power Appl.*, 11, (7), pp. 1306–1314, 2017.

[2] Y. Zhao, P. A. Crossley, and T. David, "Impact of dc bias on operating performance of current transformers," *J. Eng.*, (15), pp. 930–934, 2018.

[3] J. N. Wrubel, "Monitoring for geomagnetic induced current flow effects using existing EMS telemetering," *in Proceedings of the Power Industry Computer Application Conference*, Baltimore, pp. 45-49, 1991.

[4] K. Shetye and T. Overbye, "Modeling and analysis of GMD effects on power systems: An overview of the impact on large-scale power systems," in *IEEE Electrification Magazine*, vol. 3, no. 4, pp. 13-21, 2015.

[5] M. D. Butala *et al*., "Modeling geomagnetically induced currents from magnetometer measurements: Spatial scale assessed with reference measurements," in *Space Weather*, vol. 15, no. 10, pp. 1357-1372, 2017.

[6] P. B. Kotzé, P. J. Cilliers and P. R. Sutcliffe, "The role of SANSA's geomagnetic observation network in space weather monitoring: A review," in *Space Weather*, vol. 13, no. 10, pp. 656-664, Oct. 2015.

[7] M. Kazerooni, H. Zhu, K. Shetye, and T. J. Overbye, "Estimation of geoelectric field for validating geomagnetic disturbance modeling," *IEEE Power and Energy Conference at Illinois (PECI)*, pp. 218-224, 2013.

[8] C. Klauber and H. Zhu, "Power network topology control for mitigating the effects of geomagnetically induced currents," *50th Asilomar Conference on Signals, Systems and Computers*, CA, pp. 313-317, 2016.

[9] S. Meliopoulos, J. Xie and G. Cokkinides, "Power system harmonic analysis under geomagnetic disturbances," *18th International Conference on Harmonics and Quality of Power (ICHQP)*, pp. 1-6, Ljubljana, 2018.

[10] R. S. Girgis and K. B. Vedante, "Impact of GICs on power transformers: Overheating is not the real issue," in *IEEE Electrification Magazine*, vol. 3, no. 4, pp. 8-12, Dec. 2015.

[11] G. Swift, T. S. Molinski, R. Bray and R. Menzies, "A fundamental approach to transformer thermal modeling. II. Field verification," in *IEEE Transactions on Power Delivery*, vol. 16, no. 2, pp. 176-180, Apr 2001.

[12] K. Zheng, L. Trichtchenko, R. Pirjola and L. G. Liu, "Effects of geophysical parameters on GIC illustrated by benchmark network modeling," in *IEEE Transactions on Power Delivery*, vol. 28, no. 2, pp. 1183-1191, April 2013.

[13] R. Girgis, K. Vedante and G. Burden, "A process for evaluating the degree of susceptibility of a fleet of power transformers to effects of GIC," *IEEE PES T&D Conference and Exposition*, pp. 1-5, 2014.

[14] D. H. Boteler and R. J. Pirjola, "Modelling geomagnetically induced currents produced by realistic and uniform electric fields," *IEEE Transactions on Power Delivery*, vol. 13, no. 4, pp. 1303–1308, Oct 1998.

[15] P. Dehghanian, K. S. Shetye, K. R. Davis and T. J. Overbye, "System-Wide Case Study Assessment of Transformer Heating Due to Geomagnetic Disturbances," *North American Power Symposium (NAPS)*, Wichita, KS, USA, pp. 1-6, 2019.

[16] V. D. Albertson, J. G. Kappenman, N. Mohan, and G. A. Skarbakka, "Load-Flow Studies in the Presence of Geomagnetically-Induced Currents," *IEEE Transactions on Power Apparatus and Systems*, vol. 100, no. 2, pp. 594–607, Feb 1981.

[17] "IEEE guide for loading mineral-oil-immersed transformers," in *IEEE Std. C57.91-1995*, 1996.

[18] "Transformer thermal impact assessment white paper," North American Electric Reliability Corporation (NERC), Project 2013-03.

[19] L. Marti, A. Rezaei-Zare and A. Narang, "Simulation of Transformer Hotspot Heating due to Geomagnetically Induced Currents," *in IEEE Transactions on Power Delivery*, vol. 28, no. 1, pp. 320-327, Jan. 2013.

[20] "IEEE Guide for Loading Mineral-Oil-Immersed Transformers and Step-Voltage Regulators," in *IEEE Std C57.91-2011* (Revision of IEEE Std C57.91-1995), vol., no., pp.1-123, 7 March 2012.

[21] M. Soleimani and M. Kezunovic, "Mitigating Transformer Loss of Life and Reducing the Hazard of Failure by the Smart EV Charging," in *IEEE Transactions on Industry Applications*, vol. 56, no. 5, pp. 5974-5983, 2020.

[22] T. Tsuboi, J. Takami, S. Okabe, K. Inami and K. Aono, "Transformer insulation reliability for moving oil with weibull analysis," in *IEEE Transactions on Dielectrics and Electrical Insulation*, vol. 17, no. 3, pp. 978-983, June 2010.

[23] C. T. Gaunt and G. Coetzee, "Transformer failures in regions incorrectly considered to have low GIC-risk," *IEEE Lausanne Power Tech*, Lausanne, pp. 807-812, 2007.